Combining mathematical modelling with *in vitro* experiments to predict *in vivo* drug-eluting stent performance

Craig McKittrick[1], Sean McKee[2], Simon Kennedy[3], Keith Oldroyd[4], Marcus Wheel[5], Giuseppe Pontrelli[6], Simon Dixon[7], Sean McGinty[8,*], Christopher McCormick[1]

Abstract

In this study, we developed a predictive model of *in vivo* stent based drug release and distribution that is capable of providing useful insights into performance. In a combined mathematical modelling and experimental approach, we created two novel sirolimus-eluting stent coatings with quite distinct doses and release kinetics. Using readily measurable *in vitro* data, we then generated parameterised mathematical models of drug release. These were then used to simulate *in vivo* drug uptake and retention. Finally, we validated our model predictions against data on drug kinetics and efficacy obtained in a small *in vivo* evaluation. In agreement with the *in vivo* experimental results, our mathematical model predicted consistently higher sirolimus content in tissue for the higher dose stents compared with the lower dose stents. High dose stents resulted in statistically significant improvements in three key efficacy measures, providing further evidence of a basic relationship between dose and efficacy within DES. However, our mathematical modelling suggests a more complex relationship is at play, with efficacy being dependent not only on delivering an initial dose of drug sufficient to achieve receptor saturation, but also on the consequent drug release rate being tuned to ensure prolonged saturation. In summary, we have demonstrated that our combined *in vitro* experimental and mathematical modelling framework may be used to predict *in vivo* DES performance, opening up the possibility of an *in silico* approach to optimising the drug release profile and ultimately the effectiveness of the device.

Keywords: Drug-eluting stents, Mathematical model, *in vivo* evaluation.

*Corresponding author: Email address: sean.mcginty@glasgow.ac.uk. Tel.:
[1]Department of Biomedical Engineering, University of Strathclyde, Glasgow, UK.
[2]Department of Mathematics & Statistics, University of Strathclyde, Glasgow, UK.
[3]Institute of Cardiovascular and Medical Sciences, University of Glasgow, Glasgow, UK.
[4]Golden Jubilee National Hospital, Glasgow, UK.
[5]Department of Mechanical & Aerospace Engineering, University of Strathclyde, Glasgow, UK
[6]Istituto per le Applicazioni del Calcolo - CNR, Roma, Italy.
[7]Biomer Technology Limited, Runcorn, UK.
[8]Division of Biomedical Engineering, University of Glasgow, Glasgow, UK.

1. Introduction

Drug-eluting stents (DES) have revolutionised the treatment of coronary heart disease. The dramatic reductions in restenosis achieved with these devices, in comparison to their bare metal counterparts, now means that they are the preferred treatment option for the majority of patients requiring a coronary artery revascularisation procedure. However, they have not removed the problem of restenosis completely and around 6% of patients will need to return to hospital to undergo a costly repeat procedure within two years [1], with this rate more than doubling in high-risk patients, such as those with diabetes [2], and in complex lesions [3]. Another reported problem with currently used DES is late or very late stent thrombosis: although advanced device designs and the use of prolonged dual anti-platelet therapy now limit stent thrombosis rates to around 0.5% [1], the high mortality associated with such an event means that this remains an important clinical challenge. As a result, research efforts are currently focused on the development of next generation devices with improved safety and efficacy. A great many distinct strategies have been investigated in this pursuit, from the development of polymer-free DES to fully bioresorbable scaffolds [4]. What unites these different strategies is their combined goal of limiting restenosis, whilst ensuring optimal recovery of the endothelial cell layer. Although many different drugs have been investigated in order to selectively target smooth muscle cell proliferation whilst preserving endothelial cell function [5], few of these have reached clinical application, with current state of the art DESs generally still featuring the release of sirolimus analogues. The permanent polymers that provided prolonged drug release from the first generation Taxus and Cypher stents, have been replaced by potentially more biocompatible polymers and fully biodegradable polymer coatings. Where the first generation of DES relied on the use of stent platforms with relatively thick struts, the use of alternative metal alloys has enabled much thinner struts to be implemented in the latest platforms. The development of fully bioresorbable stent platforms is now well underway, although disappointing results from the Absorb BVS (Abbott Vascular) stent suggests that there is still further development necessary before the use of such devices becomes commonplace [6].

Most recently, there has been a return to the use of polymer-free DES, with clinical data indicating that the latest of these devices may allow the duration of anti-platelet therapy to be reduced, an effect associated with more rapid re-endothelialisation [7] [8]. Interestingly, polymer-free DES provide more rapid drug release than has typically been achieved with their polymer coated counterparts, further highlighting the importance of drug release kinetics on device performance [9]. Despite this, current research tools and models used in the optimisation of this crucial aspect of DES, remain limited in important aspects. It has long been recommended that new DES designs are subject to *in vitro* dissolution testing [10], although this is primarily to assess the consistency of the manufacturing process rather than to provide an accurate estimation of *in vivo* drug release kinetics. Moreover, such simplified models do not take account of the processes governing uptake of drug into the artery following release from the stent surface. Whilst there are some *in vitro* and *ex vivo* approaches that attempt to do this [11], ultimately animal models are still required. The value of *in vivo* models is that they most closely

mimic the clinical situation, with the pig coronary artery being the gold-standard model recommended for pre-clinical evaluation [10]. However, ethical concerns and their cost mean that they are rarely used to characterise stent drug kinetics. Even when they are employed for this purpose, they can only provide information at a limited number of time points.

It is becoming increasingly clear that *in silico* modelling can help address some of the limitations of *in vitro* and *in vivo* approaches. Such models can help to provide important insights that are not possible with these more conventional methods, thereby revealing the key mechanisms governing drug release and providing enhanced understanding of drug transport and binding processes within the vasculature [12]. For example, mathematical models have highlighted the importance of accounting for specific and non-specific binding [13] [14], concluding that for sirolimus-eluting stents it is more important to sustain release than to increase dose. Modelling has also been used to explain how differences in the binding properties of paclitaxel and sirolimus lead to different retention rates, suggesting that the optimal delivery strategy is drug-dependent [15]. Bozsak et al. [16] developed an optimisation algorithm based on a 2D-axisymmetric computational model of drug release and tissue absorption from which they concluded that paclitaxel-eluting stents require quasi-bolus or zero-order release kinetics to avoid adverse concentration levels at the endothelium, while sirolimus-eluting stents require zero-order release kinetics due to sirolimus short retention time in the arterial wall. Most recently, Tzafriri et al. [17] uncovered, through a coupled experimental and 2D computational modelling approach based on a linear dissolution-diffusion model, that deployable crystalline coatings may hold an advantage over more traditional diffusion-limited stent coatings by providing more uniform and predictable zero-order release that may be more amenable to optimisation of receptor targeting. Our own existing model, which couples a nonlinear dissolution-diffusion model of drug release from the stent surface and tissue absorption, has been shown to agree well with published experimental data generated from the Cypher stent [18]. However, in common with all other models available within the field, it relies on the estimation of a large number of parameters from *in vivo* data and thus cannot be readily used in a predictive capacity. Thus, whilst it can provide important qualitative insights into the performance of existing devices, it cannot be directly used to guide the development of new DES designs. Indeed, to the best of our knowledge, none of the current state-of-the-art models have been shown to *predict* stent drug release and tissue uptake, an important weakness that ultimately limits their utility.

In this study, we sought to develop and validate a *predictive* model of *in vivo* stent based drug release and tissue distribution. Our combined mathematical modelling and experimental approach, summarised in Figure 1, consisted of three distinct phases: *in vitro*, predictive and *in vivo*. Firstly, we created two novel sirolimus-eluting stent coatings with quite distinct doses and release kinetics. Using readily measurable *in vitro* data, we then generated parameterised mathematical models of drug release. These were then used in conjunction with a model of drug transport in the arterial wall to simulate *in vivo* drug uptake and retention. Importantly, all of the model parameters

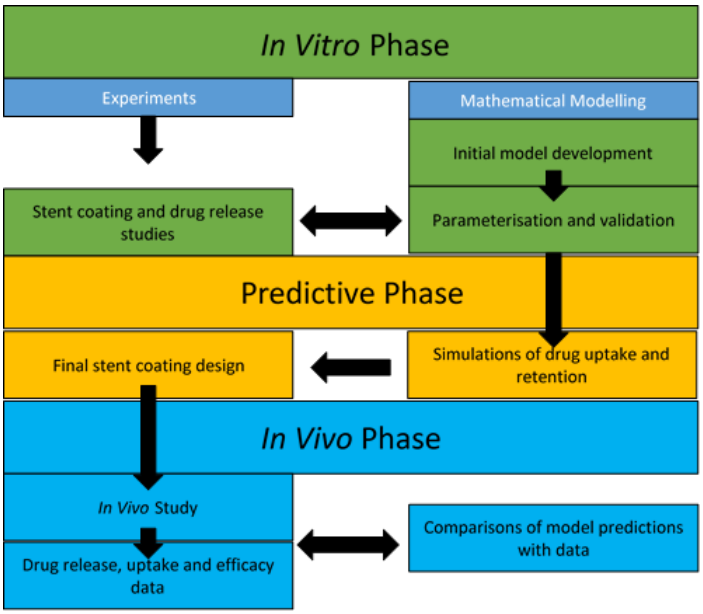

Figure 1: Schematic of our combined mathematical modelling and experimental approach.

were either generated from *in vitro* data in this study, or taken from existing literature. Finally, we validated our model predictions against data on drug kinetics and efficacy obtained in a small *in vivo* evaluation.

2. Materials and methods

2.1. Stent coating

Stent coatings were designed using a polymer developed by Biomer Technology Ltd (Runcorn, UK). The polymer, accelerate^{TM}, mimics the functional composition and distribution of the extracellular matrix integrin, arginylglycylaspartic acid (RGD), with a combination of amine, carboxylic acid and hydroxyl groups at controllable density and proportion. A drug-free stent coated with this polymer has successfully completed first-in-human safety trials [19]. Sirolimus was utilised as a model drug due to its potent anti-proliferative and immunosuppresive properties, as well as its proven success as a pharmacological agent used in DES. Sirolimus was purchased from Cfm Oskar Tropitzsch (Marktredwitz, Germany). The polymer and sirolimus were dissolved in dimethylformamide (DMF) to a final concentration of 2% (w/v), and applied as a low dose (75:25 polymer:drug) or high dose (25:75 polymer:drug) formulation. The coating was applied, using a Sono-Tek Ultrasonic Spray system (Milton, NY, USA) in a clean environment, to Flash Stents (Conic Vascular, Santiago de Compostela, Spain). Two different stent sizes were used, 14×1.8 mm for *in vitro* development and 19.3×2.5 mm for the *in vivo* study. For ease of manufacture, approximately 70% of the length of the stent was coated for *in vitro* development, whilst the entire stent was coated for the *in vivo* study. Prior to use *in vivo*, stents were crimped on to a 2.5 mm CLEVER balloon

catheter (Conic Vascular, Santiago de Compostela, Spain) using a hand crimping tool under sterile conditions.

2.2. Sirolimus release in vitro

Flash stents ($n = 2$ for each coating formulation examined [‡‡]) were coated as described above. The sirolimus release kinetics were then characterised under conditions consistent with the recommendations set out by Schwartz et al. [10]. The release medium (9 parts 0.01M phosphate buffered saline and 1-part absolute ethanol) was selected to ensure that adequate sirolimus solubility was achieved, thereby approximating an infinite sink whilst maintaining physiological relevance. All experiments were carried out in glass vials containing 1.5 ml of release medium under gyroscopic agitation at 20 rpm and 37°C. Release medium was replaced at regular sampling points of 10 minutes, 1 hour, 2 hours, 6 hours, 1 day, 3 days, 7 days, 14 days, 21 days and 28 days. At the end of the elution period, stents were immersed in methanol (4 changes of 1 ml) to strip away any remaining sirolimus. Eluent was frozen at -80°C immediately after collection. Drug release at each time point was then measured by ultraviolet spectroscopy at wavelength 278 nm (Shimadzu Corporation, Japan).

2.3. Porcine coronary stent model

The regulations, as specified by the Animals (Scientific Procedures) Act (1986), were strictly adhered to throughout and all *in vivo* experiments were performed under UK Home Office licence (Project Licence No. PPL 70/8572). Procedures were carried out on male Landrace pigs aged 85.1 ± 5.04 (mean $\pm$ standard deviation) days with a mean weight of 33 ± 3.18 kg ($n = 29$), purchased from the Scottish Rural College (Edinburgh, UK). One additional animal, aged 101 days, was used as the control tissue. The animals were allocated to three separate groups with recovery periods of 1, 7 or 28 days post-procedure. These animals were randomly assigned to receive stents with either a low dose coating or a high dose coating, implanted into the left anterior descending coronary artery (LAD), left circumflex artery (LCX) or right coronary artery (RCA). Each target vessel was restricted to the deployment of a single stent and each animal received a maximum of one of each stent type.

Animals were preloaded with dual anti-platelet drugs (aspirin 150 mg and clopidogrel 150 mg) 24 hours prior to surgery and these continued as 75 mg of each drug on alternate days post-procedurally until the termination of the experiment. Animals were sedated and anaesthetised as previously described [20]. The femoral artery was accessed using a 6 French transradial access sheath. A coronary guide catheter was used to locate the coronary ostia and a coronary wire inserted into the target vessel under radiographic guidance to identify an appropriate sized section of the vessel. The balloon was advanced over the wire and, once positioned, was inflated and held for 20 seconds, to achieve a moderate degree of injury consistent with our previous work [21]. Placement of the stent in the vessel was confirmed by radiography. Following the retrieval of access equipment,

[‡‡] n is used here and throughout to indicate the number of repeats

the femoral artery was ligated, the wound was sutured and cleaned and the animal allowed to recover.

At the termination of the experiment animals were sedated and anaesthetised as previously described [20]. Each animal was then euthanised by intravenous injection of approximately 10 ml sodium pentobarbitone (200 mg/kg). The heart was removed and stented vessels dissected and cleaned of excess fascia. The stented portion of the vessel was dissected and carefully divided into two parts to be used for histological or pharmacokinetic analysis. The proximal portion was flushed with heparinised saline and stored in 4% paraformaldehyde for 24 hours, before being transferred to 70% ethanol (in water) for longer term storage. The stent was removed from the distal portion and placed in 4 ml methanol and the tissue placed in a cryovial and flash frozen in liquid nitrogen.

2.4. Pharmacokinetics

The amount of sirolimus eluted *in vivo* was estimated by measuring the amount of the drug remaining on the stent retrieved from the distal portion of excised vessels. Stents were immersed in methanol (4 ml) and sirolimus content quantified by UV spectroscopy (278 nm). To determine the amount of intra-arterial sirolimus, a precipitation method was used. Vessel sections were ground in liquid nitrogen and then transferred to 700 μl of a 0.2 mol/l zinc sulphate in methanol solution. Each sample was vortexed at high speed for 1 minute and then centrifuged at 13000 rpm for 10 minutes. A 200 μl aliquot of the extract was taken for analysis by High Performance Liquid Chromatography (HPLC). The samples were injected onto a C-18 column in 20μl aliquots in a mobile phase of water, methanol and acetonitrile (15%:40%:45%) at a flow rate of 1 ml/min, and with UV detection at 278nm. The mass of sirolimus relative to vessel mass was calculated.

2.5. Optical coherence tomography and histology

The proximal portions of stented arteries and control tissues were initially imaged *ex vivo* by optical coherence tomography (OCT). All images were acquired by an operator blinded to the study. Arteries were submerged in 0.01 M Phosphate Buffered Saline (PBS) and a Dragonfly OCT catheter (St Jude Medical, Stratford upon Avon, UK) advanced through the vessel lumen. The entire length of the stented portion of the vessel was imaged under continuous flush of contrast-saline at 5 ml/s, and videos acquired using a Light Lab unit. From each video collected, 5 frames along the length of the stent were analysed using ImageJ software, to measure stenosis, neointimal thickness and neointimal area. Given that OCT images are dependent on operator interpretation it was also decided to perform blinded histological analysis of the artery samples. Tissue was dehydrated in ice cold acetone overnight and then embedded in glycol methacrylate (Technovit 8100, Kulzer, Wehrheim, Germany), following the manufacturer's instructions. Thin sections were cut using a Buehler Isomet 1000 rotary saw and adhered to glass microscope slides. Sections were ground to a thickness of 10 μm using a Buehler Metaserv grinder and then polished with 1500 grade sand paper. Tissue sections were stained with haematoxylin and eosin and images acquired using brightfield microscopy at x100 magnification (Nikon Eclipse E600, Tokyo, Japan). Images were analysed using

ImageJ software (National Institute of Health, Bethesda, MD, USA). Structures were manually outlined and measurements recorded for stent circumference, lumen area and the area bounded by the internal elastic lamina (IEL) and the external elastic lamina (EEL). Vessel injury score was also calculated, using a method previously described [22].

2.6. Statistical analysis

All data were assessed for normality using the Shapiro-Wilke normality test. Normally distributed data were assessed using students unpaired t-test and non-parametric data using the Mann Whitney test. All data are expressed as a mean (± standard deviation) of 2-3 sections per stent for histology and 3-5 sections for OCT. Comparisons were made using Graphpad Prism Software (La Jolla, CA, USA). Differences between groups were considered to be statistically significant when $P<0.05$.

3. Mathematical modelling

3.1. In vitro drug elution kinetics

There exists a large number of mathematical approaches for describing drug release from stents [12]. These can be roughly divided into mechanistic models and semi-empirical equations. The mechanistic models range from relatively simple approaches based on diffusion to more complex models accounting for dissolution, swelling, erosion, degradation and often a combination of two or more of these. On the other hand, in the semi-empirical approach, it is usual for drug release to be described by an equation whose terms account for observed phenomena. Where non-erodible polymer-coated stents are concerned (as in the present study), the most common approach is to assume that the dominant drug release mechanism is diffusion [12]. Our previous mathematical modelling of drug release from the Cypher stent, for example, revealed that *in vitro* drug release was well described by a simple diffusion model [23]. Others (e.g. [24]) have assumed the polymer-drug coating is a biphasic material and described two distinct modes of transport, a fast mode associated with drug release from a highly percolated structure and a slow mode resulting from the release of drug from a polymer-encapsulated phase. An example of a semi-empirical approach is the work of Tzafriri et al. [13] where a two-part equation involving an exponential and a $\sqrt{t}$ term is used to describe release of surface-connected drug and percolating drug, respectively. This biphasic approach has also been adopted in other applications, such as nickel release from an oxide layer [25].

In the present study, we test the ability of a bimodal diffusion model to describe the drug release from our novel stent coatings *in vitro*. We approximate the stent coating, of thickness L_p, as an annular region with outer radius $b = r_s + L_p$ and inner radius $a = r_s$ as is shown in Figure 2. The parameter r_s is taken to be the radius of the strut, which is assumed to be cylindrical. We further approximate the polymer/drug layer as a biphasic material with surface connected and fully embedded drug regions that are both governed by diffusive transport. We restrict our attention, as is common in the stents' literature (e.g. [12]-[13]), to a one-dimensional model. The model considers two distinct pools of drug uniformly distributed across the polymer coating. One pool of drug is released via a fast route ($c_p^{(1)}$) associated with a high diffusion coefficient ($D_p^{(1)}$) whilst

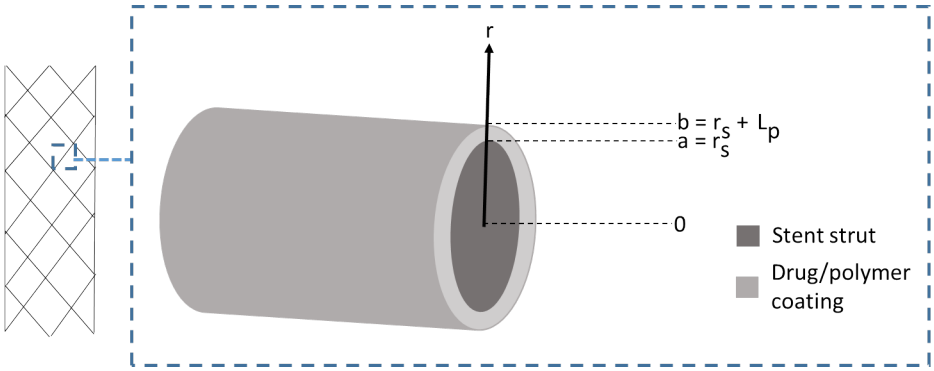

Figure 2: Schematic of cylindrical stent strut of radius r_s coated with a layer of drug/polymer occupying an annular region with outer radius $b = r_s + L_p$ and inner radius $a = r_s$.

the other is released via a slow route ($c_p^{(2)}$) associated with a low diffusion coefficient ($D_p^{(2)}$). At the stent strut/polymer coating interface ($r = a$) we assume a zero flux condition, whilst at the interface with the release medium ($r = b$), we impose an infinite sink condition, reflecting the *in vitro* experiments (Section 2.2). The model is then:

$$\frac{\partial c_p^{(i)}(r,t)}{\partial t} = D_p^{(i)}\left(\frac{\partial^2 c_p^{(i)}(r,t)}{\partial r^2} + \frac{1}{r}\frac{\partial c_p^{(i)}(r,t)}{\partial r}\right), \quad i = 1,2, \quad a < r < b, \quad t > 0, \tag{1}$$

$$-D_p^{(i)}\frac{\partial c_p^{(i)}}{\partial r} = 0, \quad i = 1,2, \quad r = a, \quad t > 0, \tag{2}$$

$$c_p^{(i)} = 0, \quad i = 1,2, \quad r = b, \quad t > 0, \tag{3}$$

$$c_p^{(i)} = C^{(i)}, \quad i = 1,2, \quad a \le r \le b, \quad t = 0, \tag{4}$$

where $C^{(1)}$ and $C^{(2)}$ are the initial uniform concentrations of drug in the respective modes, and $L_p = b - a$. This model may be solved analytically to obtain the following equation for the time-varying total mass of drug, $M(t)$, on the stent:

$$M(t) = \frac{4M_0}{b^2 - a^2}\sum_{n=1}^{\infty}\frac{f\exp\left(-\lambda_n D_p^{(1)} t\right) + (1-f)\exp\left(-\lambda_n D_p^{(2)} t\right)}{\lambda_n\left[1 - J_0^2\left(\sqrt{\lambda_n}b\right)/J_1^2\left(\sqrt{\lambda_n}a\right)\right]}, \tag{5}$$

where M_0 denotes the total initial mass of drug in the coating; f denotes the initial fraction of drug in the fast route and; J_0 and J_1 are the Bessel functions of the first kind of orders 0 and 1, respectively. Finally, λ_n is the square of the n^{th} positive root of

$$J_1\left(\sqrt{\lambda_n}a\right)Y_0\left(\sqrt{\lambda_n}b\right) - Y_1\left(\sqrt{\lambda_n}a\right)J_0\left(\sqrt{\lambda_n}b\right), \tag{6}$$

where Y_0 and Y_1 are the Bessel functions of the second kind of orders 0 and 1, respectively. It is then straightforward to derive an expression for the cumulative mass of drug released, $M_{REL}(t) = M_0 - M(t)$, henceforth referred to as the *release profile*. We

note that the more familiar 'single-mode' diffusion model may be obtained as a special case of the above model, in the limit $C^{(2)} \to 0$ (or, equivalently, $f \to 1$). The model given by (1-4) is similar to the model provided in [24], but there are two important differences. Firstly, we have chosen to employ a cylindrical coordinate system: whilst the solution to the one-dimensional diffusion equation in cartesian coordinates provides a good approximation for L_p sufficiently small, our solution is more generally applicable. Secondly, we have provided an analytical solution which offers many advantages over a purely numerical solution. For example, the analytical solution clearly displays the dependence of the release profile on the parameters of interest and allows one to observe how varying these parameters influences the release profile. With a purely numerical solution, this is not so obvious: each time the values of the parameters are changed, one has to run the simulation again.

3.1.1. Inverse estimation of bimodal diffusion model parameters

With M_0 already known from the experiments, we utilised the analytical solution (5) in conjunction with the experimental data obtained in Section 2.2 to inversely estimate the unknown parameters $D_p^{(1)}$, $D_p^{(2)}$ and f for which the model solution best fits the data. A standard least squares approach was used.

3.2. In vivo drug elution kinetics, drug content in tissue and receptor binding

Modelling drug release and tissue uptake *in vivo* is extremely challenging given the additional complexities that the *in vivo* environment introduces. As well as requiring a description of drug release from the stent, we also need equations to describe subsequent drug transport in the arterial wall. Drug release and tissue uptake occur simultaneously, and we must account for the fact that a portion of the drug released is washed away in the blood flow. In our most recent coupled model of drug release and tissue absorption [18], we modelled drug release via a dissolution-diffusion process. In the present work we instead incorporate the bimodal diffusion model to describe the drug release. In order to be able to make quantitative predictions, we approximate the DES as an equivalent phantom volume that elutes a defined drug load into the arterial wall and lumen - see Figure 3. This is similar to the approach introduced in [13], with the difference being that they modelled the stent as a phantom *surface*.

For drug transport in the arterial wall, we use the state-of-the-art nonlinear convection-diffusion-reaction model (e.g [13], [18]). We let c_w denote the volume-averaged concentration of free drug in the arterial wall of thickness L_w. Free drug may undergo diffusion with effective diffusion coefficient D_w and convection of magnitude v_w due to the transmural pressure gradient. Free drug binds reversibly to components of the tissue following saturable binding kinetics. We let b_s and b_{ns}, respectively, denote the concentration of drug that is specifically-bound (to target receptors) and non-specifically bound (to general ECM sites) in the arterial wall, with B_s and B_{ns} representing the respective binding site densities, which are assumed immobile. The rates of the forward reactions are given by k_s^f and k_{ns}^f whereas the reverse reaction rates are given by k_s^r and k_{ns}^r, where s denotes specific binding and ns denotes non-specific binding. With r_l the radius of the lumen,

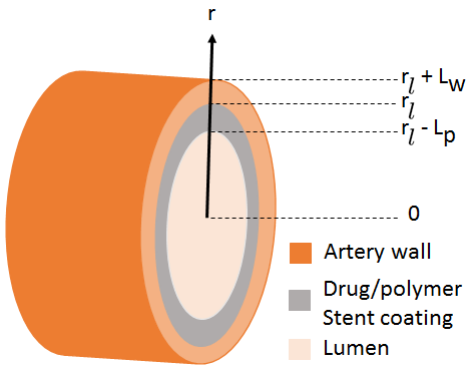

Figure 3: Schematic of DES represented as a phantom volume eluting a defined drug load M_0 into the arterial wall and lumen. The radius of the lumen is given by r_l and the parameters L_w and L_p refer to the thickness of the arterial wall and the thickness of the polymer coating, respectively.

the model of drug transport in the arterial wall is then:

$$\begin{aligned}\frac{\partial c_w^{(i)}}{\partial t} &= D_w\left(\frac{\partial^2 c_w^{(i)}}{\partial r^2}+\frac{1}{r}\frac{\partial c_w^{(i)}}{\partial r}\right)-v_w\frac{\partial c_w^{(i)}}{\partial r}\\ &\quad -k_s^f c_w^{(i)}\left(B_s-b_s^{(1)}-b_s^{(2)}\right)+k_s^r b_s^{(i)}\\ &\quad -k_{ns}^f c_w^{(i)}\left(B_{ns}-b_{ns}^{(1)}-b_{ns}^{(2)}\right)+k_{ns}^r b_{ns}^{(i)},\quad i=1,2,\quad r_l<r<r_l+L_w,\quad t>0,\end{aligned} \tag{7}$$

$$\frac{\partial b_s^{(i)}}{\partial t} = k_s^f c_w^{(i)}\left(B_s-b_s^{(1)}-b_s^{(2)}\right)-k_s^r b_s^{(i)},\quad i=1,2,\quad r_l<r<r_l+L_w,\quad t>0, \tag{8}$$

$$\frac{\partial b_{ns}^{(i)}}{\partial t} = k_{ns}^f c_w^{(i)}\left(B_{ns}-b_{ns}^{(1)}-b_{ns}^{(2)}\right)-k_{ns}^r b_{ns}^{(i)},\quad i=1,2,\quad r_l<r<r_l+L_w,\quad t>0, \tag{9}$$

where the superscript $i=1,2$ denotes drug that has emerged from the fast and slow release routes, respectively. For example, $b_s^{(2)}$ represents specifically-bound drug which has emerged from the slow release route. What remains is to couple the drug release model given by (1-2 and 4) (with $a=r_l-L_p$ and $b=r_l$), with the equations describing drug transport in the wall (7-9) to provide a coupled two-layer model. We propose the following conditions:

$$-\alpha D_p^{(i)}\frac{\partial c_p^{(i)}}{\partial r} = -D_w\frac{\partial c_w^{(i)}}{\partial r}+v_w c_w^{(i)},\quad i=1,2,\quad r=r_l, \tag{10}$$

$$c_p^{(i)} = c_w^{(i)},\quad i=1,2,\quad r=r_l. \tag{11}$$

Equation (10) is the usual statement of continuity of flux, with an important difference: the parameter α is introduced to account for some fraction of drug released from the stent being lost to the blood and therefore not reaching the arterial wall. This idea has previously been adopted in a one-layer model in the literature (e.g. [26]). Equation (11)

represents continuity of concentration of drug across the interface. Assuming the free and bound drug concentrations in the wall are zero initially:

$$c_w^{(i)} = b_s^{(i)} = b_{ns}^{(i)} = 0, \quad i = 1, 2, \quad r_l \leq r \leq r_l + L_w, \quad t = 0, \tag{12}$$

the system of equations (1-2, 4) (with $a = r_l - L_p$ and $b = r_l$) and (7-12) is then closed by allowing the concentration of free drug in the wall to vanish at the periadventitial surface (see e.g [13], [18]):

$$c_w^{(i)} = 0, \quad i = 1, 2, \quad r = r_l + L_w. \tag{13}$$

Taken together, the model equations, boundary conditions and initial conditions represent a nonlinear coupled system of 24 equations. We note that estimates of all of the parameters in the arterial wall are either available in the literature, or have been estimated from the experiments in this study prior to using the mathematical model to make predictions (Table 1) i.e. no more fitting parameters have been introduced.

Parameter	Description	Value
v_w	Magnitude of convection in arterial wall	5.8×10^{-6} cm s^{-1}
D_w	Effective diffusion coefficient in arterial wall	2.0×10^{-6} cm^2 s^{-1}
k_{ns}^f	Non-specific binding-on rate	2×10^6 $\left(\text{mol cm}^{-3}\right)^{-1}$
k_{ns}^r	Non-specific binding-off rate	5.2×10^{-3} s^{-1}
B_{ns}	Non-specific binding site density	3.63×10^{-7} mol cm^{-3}
k_s^f	Specific binding-on rate	8×10^8 $\left(\text{mol cm}^{-3}\right)^{-1}$
k_s^r	Specific binding-off rate	1.6×10^{-4} s^{-1}
B_s	Specific binding site density	3.3×10^{-9} mol cm^{-3}
L_w	Arterial wall thickness	4.5×10^{-2} cm
L_p	Polymer coating thickness	3.5×10^{-4} cm ($\star$)
A	Surface area of lumen/wall interface	1.52 cm^2 ($\star$)
r_l	Radius of lumen	1.25×10^{-1}cm ($\star$)
r_s	Radius of stent strut	3.75×10^{-3}cm ($\star$)
α	Fraction of drug lost to blood	0.01
MW	Molecular weight of sirolimus	914.172 g/mol
ρ	Density of wet arterial tissue	0.983 g/ml

Table 1: A summary of the parameter values used in the simulations. All parameters taken from [26] except those marked $\star$, which were estimated in this study prior to using the mathematical model to make predictions.

3.2.1. Model reduction

In cases where the timescale for transport in the polymer coating (T_p, approximated as $L_p^2/D_p^{(1)}$) is much greater than the timescale for transport in the arterial wall (T_w, approximated as L_w^2/D_w), i.e. $T_p/T_w >> 1$, the drug release and arterial drug transport processes may reasonably be uncoupled [27] i.e. the analytical solution for drug release (5) may be used directly as an input to the arterial wall through an appropriate flux

condition. Firstly we note that

$$\frac{dM(t)}{dt} = -\frac{4M_0}{b^2-a^2}\sum_{n=1}^{\infty}\frac{fD_p^{(1)}\exp\left(-\lambda_n D_p^{(1)}t\right)+(1-f)\,D_p^{(2)}\exp\left(-\lambda_n D_p^{(2)}t\right)}{\left[1-J_0^2\left(\sqrt{\lambda_n}b\right)/J_1^2\left(\sqrt{\lambda_n}a\right)\right]}. \quad (14)$$

Denoting the surface area of the lumen/wall interface by A, we may then write down a flux condition which ensures that a fraction α of drug which is released from the stent is transferred to the arterial wall (with the remainder lost to the blood):

$$-D_w\frac{\partial c_w}{\partial r}+v_w c_w = -\frac{\alpha}{A}\frac{dM(t)}{dt}, \quad r=r_l, \quad t\geq 0. \quad (15)$$

Therefore, in cases where $T_p/T_w >> 1$, the two-layer model given by (1-2, 4) (with $a = r_l - L_p$ and $b = r_l$) and (7-13) may be replaced with the the reduced one-layer model given by (15) together with:

$$\begin{aligned}
\frac{\partial c_w}{\partial t} &= D_w\left(\frac{\partial^2 c_w}{\partial r^2}+\frac{1}{r}\frac{\partial c_w}{\partial r}\right)-v_w\frac{\partial c_w}{\partial r} \\
&\quad -k_s^f c_w\left(B_s-b_s\right)+k_s^r b_s \\
&\quad -k_{ns}c_w\left(B_{ns}-b_{ns}\right)+k_{ns}^r b_{ns}, \quad r_l<r<r_l+L_w, \quad t>0, \quad (16)\\
\frac{\partial b_s}{\partial t} &= k_s^f c_w\left(B_s-b_s\right)-k_s^r b_s, \quad r_l<r<r_l+L_w, \quad t>0, \quad (17)\\
\frac{\partial b_{ns}}{\partial t} &= k_{ns}^f c_w\left(B_{ns}-b_{ns}\right)-k_{ns}^r b_{ns}, \quad r_l<r<r_l+L_w, \quad t>0, \quad (18)\\
c_w &= 0, \quad r=r_l+L_w, \quad t>0, \quad (19)\\
c_w &= b_s=b_{ns}=0, \quad r_l\leq r\leq r_l+L_w, \quad t=0. \quad (20)
\end{aligned}$$

3.2.2. Solution method

We used a finite difference approach to numerically solve both the coupled model given by (1-2, 4, 7-9, 10-13) and the reduced model given by (15) together with (16-20). We followed the method previously described in [18] whereby we discretize the equations spatially and then solve the resulting system of ordinary differential equations (ODE's) making use of Matlab's ODE45s solver for stiff problems (see Appendix A). The reduced model is solved in the order of 1 minute using a standard desktop computer. Details of the size of the mesh used in each case are provided in Appendix A.

4. Results and discussion

4.1. In vitro drug release

In Figure 4 we display the release profiles obtained for the low dose and high dose stents. In Table 2 we display the corresponding best fitting parameters.

We note from Table 2 that for both the high and low dose cases, the fraction of drug initially contained with the fast release mode (f) is quite different from 1, indicating that a single mode diffusion model is not appropriate to describe the release of drug

Stent	Mass of sirolimus in coating	$D_p^{(1)}$	$D_p^{(2)}$	f
Low dose	53.5 ± 0.9 μg	2.8×10^{-12} cm^2 s^{-1}	1.9×10^{-13} cm^2 s^{-1}	0.7989
High dose	110.0 ± 3.0 μg	2.2×10^{-12} cm^2 s^{-1}	7.0×10^{-14} cm^2 s^{-1}	0.4630

Table 2: A summary of the inversely estimated parameters. Note that L_p was measured to be approximately 3.5×10^{-4}cm.

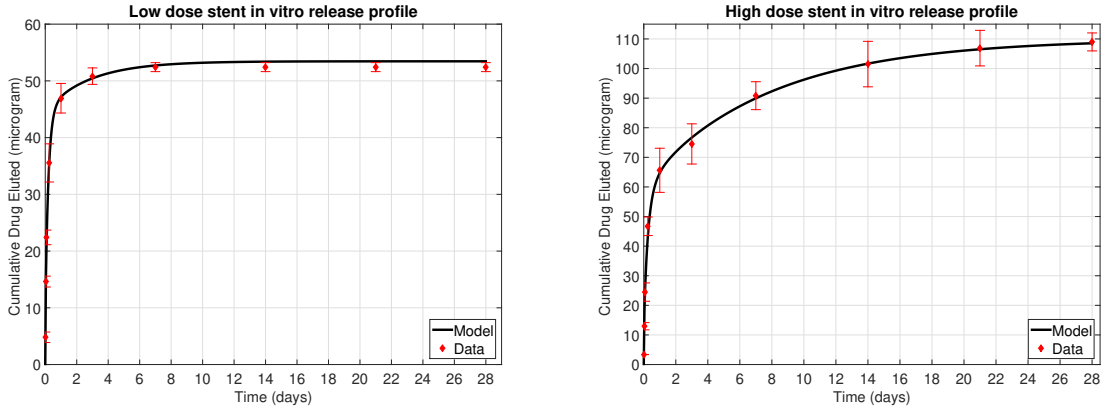

Figure 4: Low dose (left) and high dose (right) *in vitro* drug release profiles. Note the different scales on the y-axes.

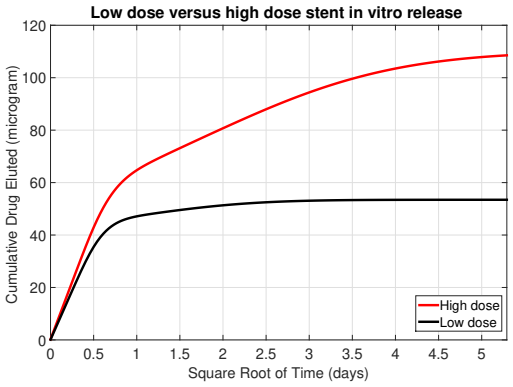

Figure 5: Low dose and high dose simulated drug release profiles plotted against $\sqrt{t}$. Low and high dose stents show distinct phases of release, with approximately linear profiles observed for the first phase when plotted against $\sqrt{t}$. The transition point between the first and second phases of drug release occurs within 1 day for both doses, but happens sooner for the low dose stent than the high dose stent.

in either case. This is further evidenced in Figure 5 where we plot the release profiles against the square root of time. The diffusion coefficients associated with the fast release route are similar for the low and high doses, whilst for the high dose case, the diffusion coefficient associated with the slow release route is an order of magnitude lower than that for the low dose case. For the low dose stent, the majority (approximately 80%) of

the drug is contained within the fast route, resulting in most of the drug being released rapidly. Within the first day, around 88% of the drug load has been released. The smaller diffusion coefficient associated with the slow route ensures that further drug is released at a much slower rate. Approximately 55% of the total high dose drug load is contained within the slow route, which coupled with the significantly lower diffusion coefficient, explains the sustained nature of the second phase of release, compared with the low dose stent. The precise reason for the differences in the parameters $D_p^{(1)}, D_p^{(2)}$ and f between the low and high dose stents is unknown. However, we expect that this is the result of the considerable differences in polymer:drug ratios between the low and high dose formulation, resulting in different drug coating transport properties.

4.2. In vivo drug elution kinetics, drug content in tissue and receptor binding

Examination of Tables 1 and 2 reveals that $T_p/T_w >> 1$ for both the low and high dose stent and so the one-layer reduced model should provide a very good approximation to the two-layer coupled model. This was verified by comparing the release profiles, drug content in tissue and saturation kinetics plots generated by both models, which were found to be indistinguishable (not shown). However, we do note that in other situations, the fully coupled two-layer model may need to be used, for example, where drug is released more rapidly from the stent, or where the drug transport in the tissue is slower. In what follows, the results presented utilise the computationally more efficient one-layer reduced model.

The best-fitting parameters of the bimodal diffusion model (Table 2) were assumed to hold *in vivo* since the same coating formulations were applied as in the *in vitro* case. However, it is noted that the *in vivo* stents were longer, resulting in a higher initial mass (M_0) than the respective *in vitro* stents. The *predictions* of the model are compared with the *in vivo* data in Figure 6. We reiterate that, due to ethical constraints, we have gathered data at only three time points which makes it impossible to completely validate the model predictions. In particular, more data points at early times would be required to fully validate the biphasic nature of the in vivo drug release profiles. However, from Figure 6 it is evident that the model's predictions are in line with the experimental data. For low dose and high dose stents, the model predicts an initial rapid release of drug over the first day, followed by a considerably slower release for the remainder of the 28 days, in line with the experimental data. We note that whilst the model is in good agreement with most of the data points, the model predicts a somewhat lower value for drug eluted at day 1 for the high dose case. Given the limited number of data points and the relatively high variability for the high dose case, it is difficult to ascertain the precise reason for this difference. For low dose and high dose stents, the model predicts a similar trend in the variation of drug content in tissue with time, i.e. an initially rapid increase to a peak within the first day followed by a steady decline over the remainder of the 28 days. Furthermore, the model predicts consistently higher drug content in tissue for the high dose stent. Both of these observations agree with the experimental data. Despite the considerable variability in the data observed for certain time points, the model is clearly capturing the key trends. One of the advantages of our model is that, as well as being able to predict drug content in tissue, we are also able to simulate drug

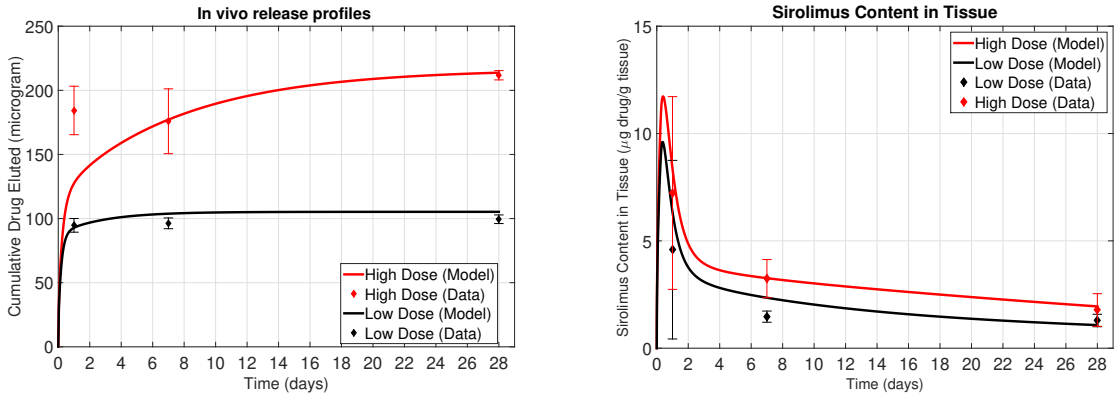

Figure 6: Comparison of model predictions with *in vivo* experimental data for low and high dose stents. Left: *in vivo* drug release profiles. Right: Drug content in arterial tissue (presented as μg drug per g of tissue) and calculated as $\frac{2}{\rho L_w(2r_l+L_w)}\int_{r_l}^{r_l+L_w} r\,(c_w+b_s+b_{ns})\,dr$, where ρ is the density of wet arterial tissue. Model simulations are given by solid lines whilst experimental data ($n=4-8$ per time point) are represented by diamonds.

binding. This is particularly useful since quantifying patterns of receptor-bound and ECM-bound drug *in vivo* is especially challenging. In Figure 7 we display simulations of target receptor and ECM binding site saturation levels, both spatially and as a function of time. From these simulations we make a number of observations. Firstly, panels A and B show that ECM binding sites do not come close to saturation over the course of the 28 days, for low dose and high dose stents. Peak ECM-bound drug levels occur within the first day and then decline rapidly thereafter (panels A and B). Secondly, low dose and high dose stents result in almost 100% target receptor saturation within 1 day (panels A and B). Thereafter, there is a steady decline which is markedly steeper for the low dose stents (panels A and B). Thirdly, beyond the first day, high dose stents (panel D) result in higher levels of target receptor saturation deeper into the arterial wall compared with low dose stents (panel C). Furthermore, beyond the first day, higher levels of receptor saturation are observed consistently for the high dose stent (panels C and D). A similar pattern is observed when considering ECM bound drug, i.e. the high dose stent results in higher % saturation levels at any given time (panels E and F). Taken together, these simulations indicate differential levels of receptor and ECM saturation between low and high dose stents, suggesting possible differences in efficacy.

4.3. in vivo morphometry

Histomorphometric analysis of excised stented arteries indicated that the higher drug dose significantly reduced the amount of neoimtima formed over 28 days compared to the low dose formulation. Indeed, all three outcome measures were significantly improved in the high dose stent group (Figure 8), despite similarly low injury scores [22] between the groups (1.05 ± 0.04 for low dose vs 1.05 ± 0.09 for high dose). Diameter stenosis was around 30% lower in the high dose arteries compared to the low dose (22.9% $\pm$ 3.7 vs 32.1% $\pm$ 5.5, P$<$ 0.04). Similarly, the area of neointimal growth was attenuated in

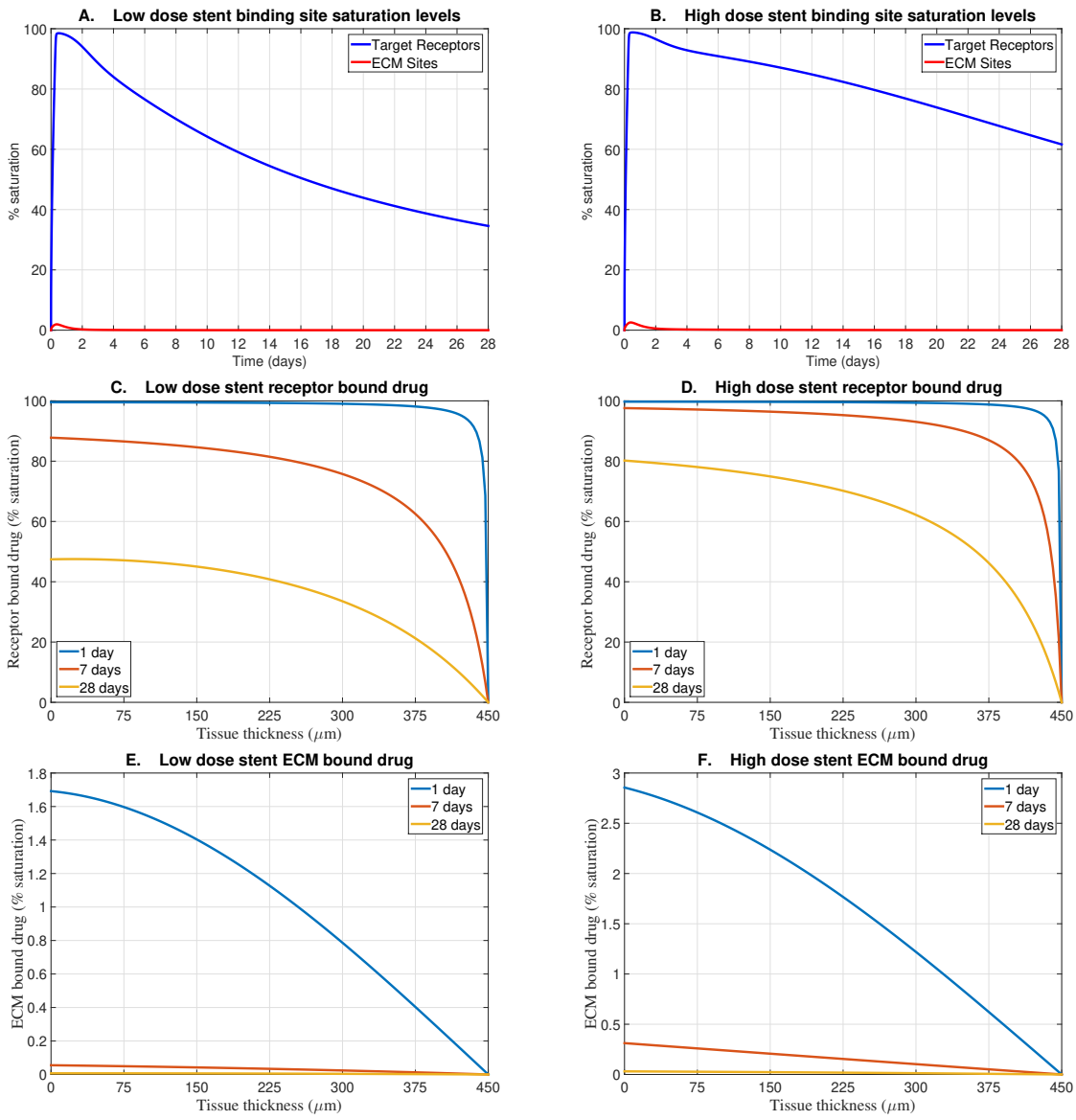

Figure 7: Model simulations of arterial drug retention and binding kinetics for low dose stents (Left panel) and high dose stents (right panel).
Upper: target receptor and ECM binding site % saturation as a function of time, calculated as $100 \times \frac{2}{B_s L_w (2r_l + L_w)} \int_{r_l}^{r_l+L_w} r b_s dr$ and $100 \times \frac{2}{B_{ns} L_w (2r_l + L_w)} \int_{r_l}^{r_l+L_w} r b_{ns} dr$, respectively. These Middle: spatial profiles of target receptor-bound drug at 1 day, 7 days and 28 days, calculated as $100 \times \frac{b_s}{B_s}$. Lower: spatial profiles of ECM-bound drug at 1 day, 7 days and 28 days, calculated as $100 \times \frac{b_{ns}}{B_{ns}}$.

the high dose group (1 mm^2 $\pm$ 0.1 vs 1.32 mm^2 $\pm$ 0.21, P$<$ 0.01), as was neointimal thickness (0.29mm $\pm$ 0.07 vs 0.44mm $\pm$ 0.07, P$<$ 0.03). Analysis of the vessels from OCT images showed a similar trend to the histological data, where all three measures were reduced in the high dose stent group though not to a statistically significant level

(Figure 9). Representative examples of stented arteries from both the high and low dose groups are shown in Figure 10.

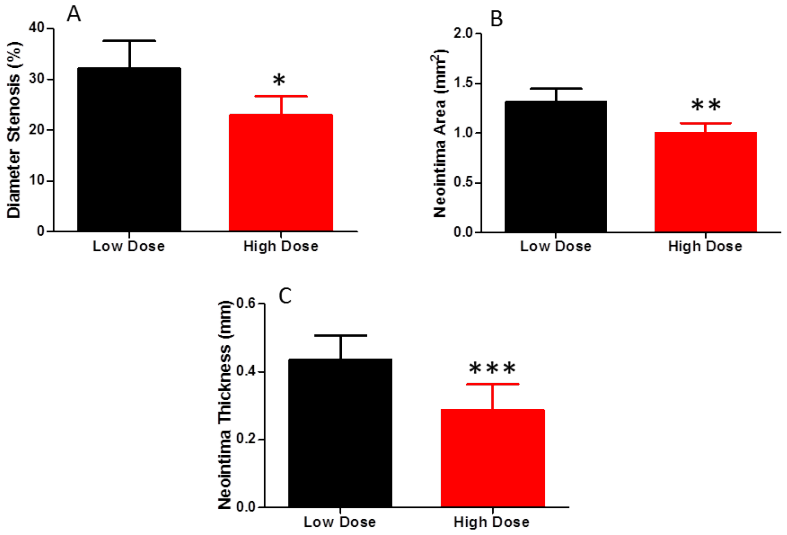

Figure 8: Histomorphometric analysis of histologically stained arterial tissue. Diameter stenosis (A), neointimal area (B) and neointimal thickness (C) from low dose (n=4) and high dose (n=4) drug eluting stents were assessed 28 days after implantation. Data are mean ± SD, $*P<0.04$, $**$ $P<0.01$ and $***$ $P<0.03$. Comparisons made using unpaired t-test.

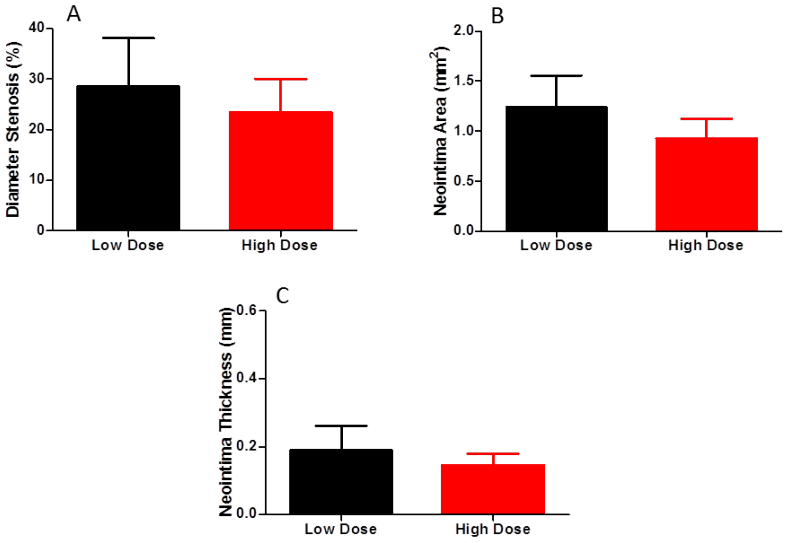

Figure 9: Histomorphometric analysis of arterial tissue imaged using optical coherence tomography. Diameter stenosis (A), neointimal area (B) and neointimal thickness (C) from low dose (n=4) and high dose (n=5) drug eluting stents were assessed 28 days after implantation. Data are mean ± SD.

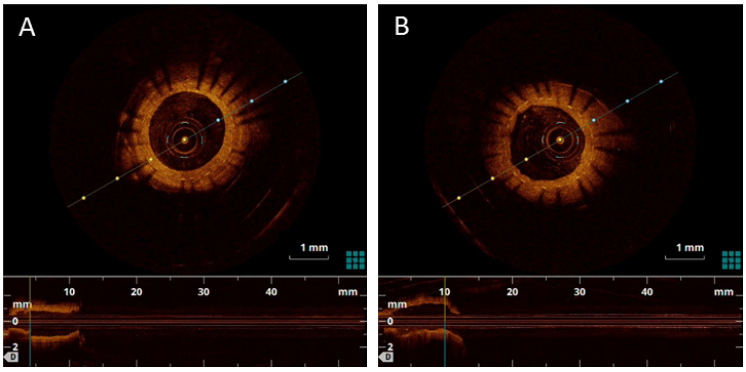

Figure 10: Images of stented coronary arteries. Arteries implanted with low dose (A) and high dose (B) drug eluting stents were imaged ex vivo using optical coherence tomography, 28 days post implantation.

5. Limitations

We would like to emphasize that there are a number of limitations in this work. Firstly, whilst we have demonstrated that a bimodal diffusion model captures the drug release well, the different model parameters associated with the high and low dose formulations points to a complex relationship between the coating composition and the drug transport parameters. We expect different coating formulations to yield different fast and slow route diffusion coefficients: our model at present is only able to infer the values of these parameters by comparison with *in vitro* data. The pursuit of more sophisticated mathematical models which are able to directly relate drug transport parameters to coating composition seems worthwhile. The use of Atomic Force Microscopy, allied to advanced spectroscopic based compositional analysis techniques, will help accelerate such advanced modelling efforts. Likewise, although the biocompatible nature of the polymer used in this study means that we expect any differences in the surface characteristics between the two stent coatings to have a comparatively small effect on our *in vivo* study observations, the use of such techniques will enable the impact of any such differences to be fully characterised. However, this does not detract from the overall aim of the work, which was to use a validated *in vitro* model of drug release to predict *in vivo* drug release and tissue absorption.

Secondly, rather than explicitly model blood flow, we (as have others [26]) have accounted for drug being lost to the blood stream through a modification of the flux boundary condition at the stent/arterial wall interface. The fraction of drug delivered to the wall (α) is likely to be dependent on the stent platform in question, in particular the geometry (i.e. surface area exposed to blood flow) and drug release kinetics. Furthermore, this parameter in reality may depend on time. The alternative is to fully account for the blood flow, which would require a more complicated higher-dimensional model. In reality, the fraction of drug lost to the blood would depend on a number of factors which would require accurate 3D stented-arterial geometries, for example the proximity of stent struts to the tissue (malapposed, protruding into the lumen, fully embedded). Such data would not be known *a priori* unless there existed a high fidelity model of

stent expansion in arteries, which of course would require an accurate description of the mechanical properties of the tissue in question.

Thirdly, there are a large number of parameters in the model. In keeping with our primary aim of making predictions, we have made use of existing published arterial wall transport parameters which have been estimated in a porcine coronary artery model, rather than finding the parameter values that best fit the data and/or performing a sensitivity analysis. These values are likely to be subject to variability, may be specific to the particular arrangements of the experiment from which they were derived and, moreover, may not be representative of the corresponding parameters in human tissue. Finally, in line with the majority of combined modelling and experimental studies in this field, we have neglected disease in this work. There is growing evidence [11] that disease composition may well have an impact on drug release and subsequent tissue distribution, which calls for the development of more advanced methodologies (both experimental and modelling) to be able to account for this.

6. Conclusions

In agreement with the *in vivo* experimental results, our mathematical model predicted consistently higher sirolimus content in tissue for the high dose stent group when compared with the low dose group. We would expect that this would result in improved efficacy, and that was indeed the case. In our *in vivo* experiments, high dose stents (c.f. low dose stents) resulted in statistically significant improvements in three key efficacy measures, seemingly supporting the idea that increased dose leads to improved efficacy. However, our mathematical modelling of drug binding kinetics paints a more complicated picture and suggests, in line with other reports [13], that dose escalation alone is not enough. Figure 6 (left) shows clearly that the high dose stents deliver more drug into the arterial wall within the first day than the low dose stents. However, model simulations (Figure 7, upper panel) suggest that in both cases, near maximal specific receptor saturation is achieved within 1 day. This may indicate that the dose of drug delivered by the low dose stent within the first day is sufficient, and that the high dose stent is delivering an unnecessarily higher dose within the same period. However, the low dose stent does not adequately provide sustained release: from Figure 6 (left) we see the release profile stagnating after the initial rapid delivery. On the other hand, the high dose stent continues to release drug for the duration of the study, providing a fresh source of drug to bind with specific receptors that have become dissociated with the drug. This sustained release ensures that the level of specific receptor saturation is higher for longer compared with the low dose case. Our findings point to the possibility of designing a stent where the dose delivered initially ensures receptor saturation is reached, but that the subsequent release is tuned to match declining receptor saturation levels, thereby acting to replenish the drug in the tissue and prolonging receptor saturation. A combined modelling and experimental approach, such as the one presented here, may well be exploited in this regard.

Acknowledgements

The authors dedicate this paper to Professor Roger Wadsworth who was instrumental in the early stages of this work, but who sadly passed away. The authors would like to acknowledge funding provided by EPSRC (Grant Nos. EP/J007242/1 and EP/J007579/1) and MRC (Grant No. MC-PC-17178).

Research Data

All experimental data created during this research are openly available from the University of Strathclyde at https://doi.org/10.15129/af09df5c-a25d-4c8c-88d9-8a6df1d8213d. The mathematical models and their solutions are detailed in the text and in the supplementary material.

Appendix A. Supplementary data

The numerical schemes are provided as supplementary data and may be found in the online version.

References

[1] R. A. Byrne, P. W. Serruys, A. Baumbach, J. Escaned, J. Fajadet, S. James, M. Joner, S. Oktay, P. Juni, A. Kastrati, G. Sianos, G. G. Stefanini, W. Wijns, and S. Windecker. Report of a european society of cardiology-european association of percutaneous cardiovascular interventions task force on the evaluation of coronary stents in europe: executive summary. *Eur. Heart J.*, 36:2608–2620, 2015.

[2] M. E. Farkouh, M. Domanski, L. A. Sleeper, F. S. Siami, G. Dangas, M. Mack, M. Yang, D. J. Cohen, Y. Rosenberg, S. D. Solomon, A. S. Desai, B. J. Gersh, E. A. Magnuson, A. Lansky, R. Boineau, J. Weinberger, K. Ramanathan, J. E. Sousa, J. Rankin, B. Bhargava, J. Buse, W. Hueb, C. R. Smith, V. Muratov, S. Bansilal, S. King, M. Bertrand, and V. Fuster. Strategies for multivessel revascularization in patients with diabetes. *N. Engl. J. Med.*, 367:2375–2384, 2012.

[3] P. W. Serruys, M. C. Morice, A. P. Kappetein, A. Colombo, D. R. Holmes, M. J. Mack, E. Stahle, T. E. Feldman, M. van den Brand, E. J. Bass, N. Van Dyck, K. Leadley, K. D. Dawkins, and F. W. Mohr. Percutaneous coronary intervention versus coronary-artery bypass grafting for severe coronary artery disease. *N. Engl. J. Med.*, 360:961–972, 2009.

[4] C. McCormick. 1- overview of cardiovascular stent designs. In J. Gerard Wall, H. Podbielska, and M. Wawrzynska, editors, *Functionalised Cardiovascular Stents*, chapter 1, pages 3–26. Woodhead Publishing, 2018.

[5] R. Tang and S. Y. Chen. Smooth muscle-specific drug targets for next-generation drug-eluting stent. *Expert Rev. Cardiovasc. Ther.*, 12:21–23, 2014.

[6] S. Bangalore, E. R. Edelman, and D. L. Bhatt. First-generation bioresorbable vascular scaffolds: Disappearing stents or disappearing evidence? *J. Am. Coll. Cardiol.*, 69:3067–3069, 2017.

[7] D. Carrie, I. Menown, K. Oldroyd, S. Copt, S. Talwar, L. Maillard, M. C. Morice, L. S. Teik, I. Lang, and P. Urban. Safety and efficacy of polymer-free biolimus a9-coated versus bare-metal stents in orally anticoagulated patients: 2-year results of the leaders free oral anticoagulation substudy. *JACC Cardiovasc. Interv.*, 10:1633–1642, 2017.

[8] R. Waksman, G. N. Piegari, A. Kabour, L. C. on, G. Adams, N. Solankhi, A. Smeglin, D. J. Kereiakes, R. Leiboff, M.-A. Spad, R. Torguson, N. Chandra, R. Bastian, J. Degroot, M. W. Kayo, H.-P. Stoll, and H. M. Garcia-Garcia. Polymer-free biolimus a9-coated stents in the treatment of de novo coronary lesions with short dapt: 9-month angiographic and clinical follow-up of the prospective, multi-center biofreedom USA clinical trial. *Cardiovasc. Revasc. Med.*, 18:475–481, 2017.

[9] M. I. Papafaklis, Y. S. Chatzizisis, K. K. Naka, G. D. Giannoglou, and L. K. Michalis. Drug-eluting stent restenosis: Effect of drug type, release kinetics, hemodynamics and coating strategy. *Pharmacol. Ther.*, 134:43–53, 2012.

[10] R. S. Schwartz, E. Edelman, R. Virmani, A. Carter, J. F. Granada, G. L. Kaluza, N. A. F. Chronos, K. A. Robinson, R. Waksman, J. Weinberger, G. J. Wilson, and R. L. Wilensky. Drug-eluting stents in preclinical studies: Updated consensus recommendations for preclinical evaluation. *Circ. Cardiovasc. Interv.*, 1:143–153, 2008.

[11] C. M. McKittrick, S. Kennedy, K. G. Oldroyd, S. McGinty, and C. McCormick. Modelling the impact of atherosclerosis on drug release and distribution from coronary stents. *Ann. Biomed. Eng.*, 44:477–487, 2015.

[12] S. McGinty. A decade of modelling drug release from arterial stents. *Math. Biosci.*, 257:80–90, 2014.

[13] A. R. Tzafriri, A. Groothuis, G. Sylvester Price, and E. R. Edelman. Stent elution rate determines drug deposition and receptor-mediated effects. *J. Control. Release*, 161:918–926, 2012.

[14] S. McGinty and G. Pontrelli. On the role of specific drug binding in modelling arterial eluting stents. *J. Math. Chem.*, 54:967–976, 2016.

[15] F. Bozsak, JM Chomaz, and A. I. Barakat. Modeling the transport of drugs eluted from stents: physical phenomena driving drug distribution in the arterial wall. *Biomech. Model. Mechanobiol.*, 13(2):327–347, 2014.

[16] F. Bozsak, D. Gonzalez-Rodriguez, Z. Sternberger, P. Belitz, T. Bewley, J-M Chomaz, and A. I. Barakat. Optimization of drug delivery by drug-eluting stents. *PLoS ONE*, 10(6):e0130182, 2015.

[17] A. R. Tzafriri, F. Garcia-Polite, X. Li, J. Keating, J-M. Balaguer, B. Zani, L. Bailey, P. Markham, T. C. Kiorpes, W. Carlyle, and E. R. Edelman. Defining drug and target protein distributions after stent-based drug release: Durable versus deployable coatings. *J. Control. Release*, 274:102–108, 2018.

[18] S. McGinty and G. Pontrelli. A general model of coupled drug release and tissue absorption for drug delivery devices. *J. Control. Release*, 217:327–336, 2015.

[19] N. Kipshidze, A. Archavdze, V. Kipiana, M. Kantaria, T. Gunjun, S. Khurtzidze, and R. Erbel. New polymeric biomaterial acceleratetm-at coated stent: First-in-man clinical study 2 year results. *9th International Congress on Coronary Artery Disease, International Proceedings*, pages 391–394, 2011.

[20] A. Ialenti, G. Grassia, P. Gordon, M. Maddaluno, M. V. Di Lauro, A. H. Baker, A. Guglielmotti, A. Colombo, G. Biondi, S. Kennedy, and P. Maffia. Inhibition of in-stent stenosis by oral administration of bindarit in porcine coronary arteries. *Arterioscler. Thromb. Vasc. Biol.*, 31:2448–2454, 2011.

[21] J. Watt, S. Kennedy, C. McCormick, E. O. Agbani, A. McPhaden, A. Mullen, P. Czudaj, B. Behnisch, R. M. Wadsworth, and K. G. Oldroyd. Succinobucol-eluting stents increase neointimal thickening and peri-strut inflammation in a porcine coronary model. *Catheter. Cardiovasc. Interv.*, 81:698–708, 2013.

[22] J. Gunn, N. Arnold, K. H. Chan, L. Shepherd, D. C. Cumberland, and D. C. Crossman. Coronary artery stretch versus deep injury in the development of in-stent neointima. *Heart*, 88:401–405, 2002.

[23] S. McGinty, S. McKee, R. M. Wadsworth, and C. McCormick. Modeling arterial wall drug concentrations following the insertion of a drug-eluting stent. *SIAM J. Appl. Math.*, 73(6):2004–2028, 2013.

[24] S. Hossainy and S. Prabhu. A mathematical model for predicting drug release from a biodurable drug-eluting stent coating. *J. Biomed. Mater. Res. Part A*, 87:487–493, 2008.

[25] D.M. Saylor, L. Adidharma, J.W. Fisher, and RP Brown. A biokinetic model for nickel released from cardiovascular devices. *Regul. Toxicol. Pharmacol.*, 80, 2016.

[26] N. Artzi, A. R. Tzafriri, K. M. Faucher, G. Moodie, T. Albergo, S. Conroy, S. Corbeil, P. Martakos, R. Virmani, and E. R. Edelman. Sustained efficacy and arterial drug retention by a fast drug eluting cross-linked fatty acid coronary stent coating. *Ann. Biomed. Eng.*, 44(2):276–286, 2016.

[27] T. Vo, W. Lee, A. Peddle, and M. Meere. Modelling chemistry and biology after implantation of a drug-eluting stent. part i: Drug transport. *Math. Biosci. Eng.*, 14:491–509, 2017.